

Bernard J. Geurts

**Direct and Large-Eddy Simulation**

# **De Gruyter Series in Computational Science and Engineering**



Edited by

Eric Darve, Stanford, USA

George Em Karniadakis, Providence, USA

Houman Owhadi, Pasadena, USA

## **Volume 1**

Bernard J. Geurts

# **Direct and Large-Eddy Simulation**

---

**DE GRUYTER**

**Mathematics Subject Classification 2020**

35Lxx, 35Qxx, 65Dxx, 65Mxx, 76D05, 76Fxx, 76N10

**Author**

Prof. Dr. Bernard J. Geurts

University of Twente

Department of Applied Mathematics

PO Box 217

7500 AE Enschede

The Netherlands

Eindhoven University of Technology

Multiscale Physics of Energy Systems

PO Box 513

5600 MB Eindhoven

The Netherlands

b.j.geurts@utwente.nl

ISBN 978-3-11-051621-0

e-ISBN (PDF) 978-3-11-053236-4

e-ISBN (EPUB) 978-3-11-053182-4

ISSN 2512-7276

**Library of Congress Control Number: 2022944170**

**Bibliographic information published by the Deutsche Nationalbibliothek**

The Deutsche Nationalbibliothek lists this publication in the Deutsche Nationalbibliografie; detailed bibliographic data are available on the Internet at <http://dnb.dnb.de>.

© 2023 Walter de Gruyter GmbH, Berlin/Boston

Typesetting: VTeX UAB, Lithuania

Printing and binding: CPI books GmbH, Leck

[www.degruyter.com](http://www.degruyter.com)

---

To Vincent, Lennart and Elisabeth



# Preface

Direct and large-eddy simulations of turbulent flow form the subject of this book. These simulation strategies are focused on capturing the primary features of unsteady flow through computation. In direct numerical simulation, the governing equations are represented numerically with sufficiently high temporal—and spatial—resolution to capture all dynamically relevant flow features. The basis for large-eddy simulation is somewhat different in nature. Next to an element of numerical modeling, the large-eddy approach is characterized by an element of mathematical–physical modeling to account for the desired coarsening of the description.

A major step in the large-eddy approach consists of the smoothing and regularization of the dynamical complexities of the full flow equations. This is achieved through some form of explicit or implicit filtering. A closure problem arises as a consequence of the filtering that introduces the element of modeling into the simulation strategy. In fact, an external length-scale, identified with the width of the filter, is introduced, that offers control over the smallest features in the flow description. The dynamical effects of flow structures that are smaller than this filter-width constitute the closure problem which needs to be properly parameterized through the explicit introduction of a so-called subgrid model. Here, a combination of understanding of turbulence, mathematical structure preservation and the use of data available from the flow problem at hand is crucial. This entails phenomenological models that are meant to yield simulation results of ‘sufficient accuracy’ and at ‘much reduced computational costs’. These two qualitative indications, i. e., ‘sufficient accuracy’ and ‘much reduced computational costs’, are at the core of this book—these concepts will be quantified generically as well as in their problem-specific context in various ways.

The search for a proper and acceptable balance between the reduction of information contained on the one hand, while retaining sufficient accuracy on the other hand, are recurring topics in this book and express themselves, e. g., in attention to the mathematical properties of the modeling process, the development of accurate numerical methods, the construction of suitable subgrid models to represent the dispersive and dissipative effects of small-scale turbulence and the analysis of the interaction between discretization and modeling errors that complicate the interpretation and reliability of actual large-eddy simulations.

The material in this book is organized into four parts. In the first part, some basic phenomenology of turbulence is described, together with the governing equations and the introduction of the filtered flow representation. The second part addresses the main numerical elements associated with direct and large-eddy simulation, i. e., the time-integration and the spatial discretization. Subgrid modeling is discussed in the third part, including the mathematical–physical aspects of the modeling process as well as a collection of basic—and more involved subgrid models. Finally, in the fourth part, the central validation and interacting error dynamics are illustrated.

This book has arisen from courses that were given in recent years for PhD students of the J.M. Burgers Center, a research school for fluid dynamics in the Netherlands, lectures compiled in the context of an ERCOFTAC summer school (European research community for flow, turbulence and combustion), e. g., in Krakow (Poland), in Trieste (Italy), in the context of the ANIMATE project headed by the University of Czestochowa (Poland) and in lectures for BIMOS – the Berlin International Graduate School in Model and Simulation Based Research. The emphasis has been put on making the basic problem areas in large-eddy simulation transparent and accessible. It is hoped that this book provides a clear overview, as well as easy access to this more specialized literature. This book is an updated and extended exposition of the earlier ‘Elements of Direct and Large-Eddy Simulation’ [65].

This book aims to appeal to academic researchers as well as CFD practitioners in industry. It is intended for PhD candidates and can also be used as a textbook at the level of MSc (or MEng) studies in engineering, applied mathematics and physics. It is hoped that this book provides a good introduction to large-eddy simulation as well as stimulation for further research into numerical methods and turbulence modeling, and their application in technology and natural sciences.

Bad Bentheim, October 23, 2022

Bernard J. Geurts

# Contents

Preface — VII

## Part I: Phenomenology of turbulent flow

- 1 Direct and large-eddy simulation: context and introduction — 3**
  - 1.1 Introduction — 3
  - 1.2 Navier–Stokes equations for (in)compressible flow — 7
  - 1.3 Complexity reduction: options and limitations — 16
  - 1.4 Filtering the Navier–Stokes equations — 24
  - 1.5 An overview of DNS and LES capabilities — 32
  
- 2 Computational dynamical systems for turbulence — 38**
  - 2.1 Introduction — 38
  - 2.2 Physical space realizations of turbulent flow — 41
  - 2.3 Spectral view of turbulence — 47
  - 2.4 Dynamical systems interpretation of large-eddy modeling — 53
  - 2.5 Canonical flows as a testing ground — 57
    - 2.5.1 Homogeneous isotropic turbulence — 58
    - 2.5.2 Turbulence in mixing layers — 60
    - 2.5.3 Wall-bounded turbulent flow — 63

## Part II: Numerical aspects of DNS and LES

- 3 Features of a basic numerical approach — 67**
  - 3.1 Introduction — 67
  - 3.2 Basic approaches to discretization — 69
  - 3.3 Accuracy and stability of numerical methods — 74
  - 3.4 Templates for compressible and incompressible flow solvers — 81
  
- 4 Time-integration — 87**
  - 4.1 Introduction — 87
  - 4.2 Explicit time-integration — 89
  - 4.3 Implicit time-integration — 95
  - 4.4 Solving linear systems — 100
  - 4.5 Determination of an accuracy time-step — 104
  
- 5 Spatial discretization — 110**
  - 5.1 Introduction — 110

- 5.2 Finite difference methods and numerical quadrature — 112
- 5.3 Finite volume methods — 126
- 5.4 Implicit compact differencing methods — 136
- 5.5 Spectral methods — 140
- 5.6 Boundary conditions — 148
- 5.7 Validation using stability theory — 157

### Part III: Subgrid modeling

- 6 Filtering and rigorous subgrid modeling — 167**
  - 6.1 Introduction — 167
  - 6.2 Basic and high-order filters in large-eddy simulation — 169
  - 6.3 Realizability conditions for the turbulent stresses — 178
  - 6.4 Approximate inverse modeling — 181
  - 6.5 Algebraic properties of turbulent stresses — 189
  - 6.6 Estimates for the commutator-errors — 191
  - 6.7 Regularization principles — 196
- 7 Subgrid models — 200**
  - 7.1 Introduction — 200
  - 7.2 Basic modeling of the turbulent stress-tensor — 202
  - 7.3 Dynamic and inverse modeling of turbulent stresses — 216
  - 7.4 Wall modeling — 222
  - 7.5 Compressibility effects on subgrid scale — 226
  - 7.6 Commutator-error modeling — 230

### Part IV: Validation and error-assessment

- 8 Validation of large-eddy simulation — 237**
  - 8.1 Introduction — 237
  - 8.2 A priori testing — 239
  - 8.3 A posteriori testing — 242
  - 8.4 Validation of large-eddy simulation of a mixing layer — 245
  - 8.5 Validation of boundary layer flow — 253
- 9 Interacting error dynamics — 258**
  - 9.1 Introduction — 258
  - 9.2 A priori estimates of discretization error effects — 261
  - 9.3 Grid dependence of large-eddy predictions — 263
  - 9.4 Interactions between errors and LES paradoxes — 269

9.5 Predicting accuracy limitations in LES — 273

10 Epilogue — 289

Bibliography — 295

Index — 305



---

## Part I: **Phenomenology of turbulent flow**



# 1 Direct and large-eddy simulation: context and introduction

**Abstract:** A global introduction to direct and large-eddy simulation is given. The governing equations of fluid flow are introduced and some of their mathematical and physical background is discussed. A short phenomenology of basic turbulent flow features is presented. This provides a pragmatic justification for the general framework of so-called reduced-flow descriptions. These descriptions are aimed at capturing the primary properties of turbulent fluid flow and are obtained by suitably reducing the dynamical complexity of the underlying governing equations. In particular, the basis for large-eddy simulation is obtained by spatially filtering the system of flow equations. The central closure problem that arises from this filtering is identified and an overview of the capabilities and limitations of direct and large-eddy simulations is sketched.

## 1.1 Introduction

Simulation strategies that are focused on strongly unsteady turbulent flow phenomena have grown tremendously in importance over the past few decades [73, 152, 179, 181]. The renowned and seemingly unpredictable state of turbulent fluid flow has become more accessible to large-scale numerical simulation and modeling studies. This has been made possible due to three main developments, i. e., increased computational capabilities of modern computers, improvements in accuracy and efficiency of numerical methods and advances in modeling turbulent flow features. In this book, we will concentrate on the latter two elements and describe numerical methods and small-scale turbulence modeling of relevance to complex turbulent flows.

Two closely related simulation strategies form the central objective are: direct numerical simulation (usually denoted by the acronym DNS) and large-eddy simulation (known by the acronym LES). In the DNS approach one aims to solve the full system of well-established fluid flow equations without any further approximations other than of a numerical nature. In this respect one may think of, in principle, well-controllable numerical effects associated with, e. g., discretization method, spatial resolution, flow geometry representation and boundary conditions. The large-eddy simulation approach involves, in addition, a reduction of the dynamical complexity, e. g., by spatial convolution filtering employing a low-pass filter and the treatment of the corresponding closure problem [106, 125, 126, 144, 171, 187].

### Filtering and closure

With the use of a low-pass filter operation, one may effectively remove those features from the flow description that are smaller than the so-called width of the filter  $\Delta$ . Si-

multaneously, the filter leaves structures larger than  $\Delta$  basically unaffected. Consequently, the filtering results in a significant smoothing of a flow field on scales below  $\Delta$ , while retaining the main structures that are larger than  $\Delta$ . The filter-width  $\Delta$  represents an externally specified characteristic length-scale in the large-eddy formulation of any flow problem, next to the length-scales associated with the flow geometry of the problem considered and the fundamental length-scales corresponding to the flow conditions.

The explicit filtering of the nonlinear terms in the governing equations gives rise to a central closure problem in the large-eddy formulation [58]. This closure problem is defined with direct reference to the adopted filter operation [70]. To characterize this relation between filter and closure problem, the filter-width  $\Delta$  is an important parameter. In fact, to obtain a viable large-eddy flow description, the unclosed filtered equations require the modeling of the dynamic consequences of all turbulent flow features that are smaller than  $\Delta$ . This is achieved through the introduction of a so-called ‘subgrid model’. In particular, the required model for the ‘sub- $\Delta$ ’ flow features needs to be formulated solely in terms of the filtered flow solution in order to arrive at a ‘closed’ description. The reduced dynamic complexity and associated reduced computational costs, i. e., the extended range of applicability of LES compared to DNS, constitute the main virtues of the large-eddy approach. Simultaneously, the modeling of the filtered nonlinear terms that make up the closure problem represents the primary challenge.

The DNS and LES simulation strategies are closely related. On the one hand, in direct numerical simulation, the complete turbulent solution is obtained once all features are numerically approximated in a well-controlled fashion. On the other hand, in large-eddy simulation, a solution to the filtered governing equations is the final goal. The amount of detail contained in the large-eddy solution and the burden put on the small-scales turbulence modeling depend largely on  $\Delta$ . In particular, if  $\Delta$  tends to zero, a gradual convergence from LES to DNS should arise since the filtering becomes less and less effective within this limit. A relevant parameter that measures the dynamic importance of the sub- $\Delta$  flow features is the ratio between  $\Delta$  and the smallest fundamental turbulent length-scale  $\eta$  characterizing the finest dynamically relevant details in a DNS solution. Usually, the so-called Kolmogorov length-scale [112] is selected for  $\eta$ .

### Crossover from LES to DNS

The crossover from a strongly reduced LES description at sizeable  $\Delta/\eta$  to a ‘well-resolving’ LES at smaller  $\Delta/\eta$  and finally to a full-scale DNS as  $\Delta/\eta \leq \mathcal{O}(1)$ , identifies the LES approach as a so-called ‘rational’ modeling approach to turbulent flow simulation. By ‘rational’ we imply that the fully detailed description (DNS) is contained as a limiting case in a family of reduced descriptions (LES). The ‘normalized’ filter-width  $\Delta/\eta$ , or the filter-width  $\Delta$  itself, can be used as label for the ‘members’ in the LES

family. This label identifies a measure for the ‘distance’ by which a particular LES is separated from the corresponding DNS. In this way, the large-eddy approach is seen to be a perturbation of the full direct simulation approach.

This interpretation of the large-eddy approach allows, in principle, simple control over the error that may arise in a large-eddy simulation. In fact, by suitably adjusting the filter width  $\Delta$  the ‘distance’ with respect to the corresponding direct simulation can be controlled. If we ignore numerical complications for the moment, the accuracy with which a certain (statistical) quantity needs to be predicted determines an upper bound for  $\Delta/\eta$  for each specific subgrid model. Development of a large-eddy simulation should include at least the search for a balance between the advantageous reduction of the computational costs on the one hand and dealing with the corresponding reduction of information content in the smoothed solution on the other hand.

The crossover between LES and DNS that arises by reducing  $\Delta$  also explains many of the similarities in techniques, challenges and problems associated with these simulation strategies. It forms the main motivation for discussing them in a single book. In order to appreciate these simulation strategies, two main elements emerge. First, a detailed knowledge of numerical methods, such as temporal and spatial discretization, and of their effective processing on present-day computers is required. Second, limitations in computational capabilities, as well as the required detail of flow information, may introduce the option of reducing the completeness of the flow description. The latter implies less computational effort but also introduces the element of having to model turbulent flow features. In addition, the combination of numerical methods and specific small-scale turbulence modeling within any simulation approach creates the opportunity for interaction between these two elements, especially at a marginal spatial resolution. This may significantly complicate the LES interpretation and robustness.

### **Computational dynamical system**

The final computational dynamical system that arises from the numerical and physical modeling is a complex model whose dynamical features are designed to mimic the characteristic aspects of the fluid flow. Whether this mimicking has actually been achieved and to what extent this is actually required is a matter of precise and systematic assessment of flow predictions arising from the complete computational models. Specific, application-related requirements usually play an important role in this assessment. Because of the nonlinear interactions between elements of mainly numerical, or of a mainly turbulence modeling nature, and the unknown long-time accumulation of these effects, a significant role for systematic validation is unavoidable [67, 68, 232].

In order for LES to be computationally effective, the predefined length-scale  $\Delta$  must be much larger than the smallest turbulent length scales in the flow. The corre-

sponding significant smoothing then induces a substantial reduction in the effective degrees of freedom. Typically, this also implies a sizeable deviation between the LES predictions of the smallest retained scales of order  $\Delta$  and filtered DNS predictions of flow features with the same scales. Hence, a close correspondence between instantaneous snapshots of LES and filtered DNS solutions is not likely for all scales. Still, the smoothing effects may be much more modest for a number of ‘derived’ flow properties such as mean-flow and statistical fluctuation predictions. In this way, the resulting computational dynamical systems can play their role in capturing the primary flow features, despite the inherent deviations that may arise in relation to predicting the instantaneous smallest scales.

### **Turbulence, theory and experiment**

The study of turbulent flows has a long relationship with applied mathematics and theoretical physics. Extensive (approximate) analytical theory has been and continues to be developed and eventually a feeling of ‘understanding’ of fluid flow can arise only from these approaches. However, the complexity of turbulence strongly limits progress. Therefore, physical experiments and simulation are the only direct alternatives to guide and underpin further theoretical developments. Moreover, experiments and simulation can provide invaluable information in various technological application areas, in biology, geophysical flows etc. and support engineering and design activities.

Experimental research has been and will remain of fundamental importance in this field, for example through physical-scale experiments. In particular, recent developments in nonintrusive field measurements such as Particle Image Velocimetry (PIV), Particle Tracking Velocimetry (PTV) and related approaches will supply a precise impression of unsteady (coherent) flow details [171]. This will create new opportunities for validation as well as application of DNS and LES. The simulation approach can be advantageous over actual experiments when many flow quantities at a single instance are needed. Moreover, sometimes one may attempt to obtain quantities that are difficult to measure or perform experiments under extreme conditions that are hard to represent experimentally, e. g., at high velocities such as in aerodynamics, at high temperatures such as in combustion, those involving hazardous substances such as in nuclear engineering or at large scales such as in astronomy or geophysics. Although simulations may be advantageous under these conditions, care must be taken to properly validate and assess the simulation approach and to use it as much as possible as a complementary technique, side by side with physical experiments.

It is the purpose of this book to give an introduction to the direct and large-eddy simulation strategies, to arrive at a sufficiently varied intuitive understanding of their potentials and limitations and to develop a constructive capability to formulate relevant validation and verification approaches to assess the quality of specific compu-

tations. Particular interest will hence be given to numerical methods, to turbulence modeling and to their dynamic interaction. These elements constitute the backbone of this book.

The organization of this chapter is as follows. In section 1.2 the governing equations will be identified and scaled to yield the basic dimensionless description of fluid flow used as the starting point for DNS and LES. Some basic properties of these equations are sketched in Section 1.3 to identify a context for reduced descriptions. In Section 1.4 the spatial filtering of the equations will be described in a somewhat more quantitative way and the full-closure problem will be specified. An overview of DNS–LES capabilities and limitations is provided in Section 1.5.

## 1.2 Navier–Stokes equations for (in)compressible flow

In this section, we will introduce the Navier–Stokes equations for incompressible flow in dimensional form and subsequently render these equations dimensionless. Moreover, we introduce the corresponding Kelvin circulation theorem and discuss some basic transformation properties. In addition, we specify the one-dimensional Burgers equation which is an important model equation illustrating some basic properties of the complete Navier–Stokes system. Following this, we extend the incompressible formulation and describe the compressible flow equations. We will also sketch several further extensions that involve external forces, e. g., such as gravity, or solid-body rotations. Finally, we introduce passive and active scalar equations. These scalar fields can be used to model, e. g., buoyancy-driven flows such as may be encountered in numerous geophysical applications or to describe combustion and heat-release processes. This provides a point of reference for a variety of illustrations later on in the book.

### Incompressible fluids

The starting point for the numerical simulation of fluid flow is formed by Newton's equations of motion for a continuous medium. If a fluid is considered to be incompressible, then its state of motion can be described by  $\{u_i^*, p^*\}$ , where  $u_i^*$  denotes the Cartesian velocity component in the  $x_i^*$  direction and  $p^*$  is the pressure. Here,  $i$  runs from 1 to  $d$ , where  $d$  is the dimension of the problem. We label quantities that have a physical dimension with an asterisk and express the governing equations in their dimensional form first.

In three spatial dimensions, the four fields  $\{u_i^*, p^*\}$  may be dependent on location  $\mathbf{x}^* = [x_1^*, x_2^*, x_3^*]$  and time  $t^*$ . Many good textbooks exist that give a detailed account of the phenomenological modeling involved in the governing equations for fluid flow, known as the Navier–Stokes equations [53, 91, 125]. The final set of equations repre-

sents the physical concepts of conservation of mass and momentum and can be written as:

$$\frac{\partial u_j^*}{\partial x_j^*} = 0 \quad (1.1)$$

$$\frac{\partial u_i^*}{\partial t^*} + \frac{\partial(u_i^* u_j^*)}{\partial x_j^*} + \frac{\partial(p^*/\rho^*)}{\partial x_i^*} - \nu^* \frac{\partial^2 u_i^*}{\partial x_j^{*2}} = 0 \quad (1.2)$$

for  $i = 1, 2, 3$ . Here,  $\nu^*$  denotes the kinematic viscosity  $\nu^* = \mu^*/\rho^*$ , where  $\mu^*$  is the viscosity and  $\rho^*$  the (constant) fluid density. In these equations the continuity equation (1.1) represents conservation of mass and (1.2) represents conservation of momentum. Throughout this book, we will use the summation convention for repeated indices. As an example, in this notation we have

$$\frac{\partial u_j^*}{\partial x_j^*} = \frac{\partial u_1^*}{\partial x_1^*} + \frac{\partial u_2^*}{\partial x_2^*} + \frac{\partial u_3^*}{\partial x_3^*} = \nabla^* \cdot \mathbf{u}^* = \text{div}^*(\mathbf{u}^*) = 0, \quad (1.3)$$

where  $\nabla^* = [\partial/\partial x_1^*, \partial/\partial x_2^*, \partial/\partial x_3^*]$  and  $\text{div}^*$  denotes the divergence operator. This example illustrates how one can transfer from the selected notation to other notations frequently used in the literature.

In order to facilitate a comparison between seemingly different flow problems and to help the interpretation of trends in observed flow behavior as a function of variations in physical parameters, it is helpful to render the equations (1.1) and (1.2) dimensionless. If we identify the physical dimensions that play a role in incompressible flow problems we notice that mass, length and time arise. With properly selected reference variables, the Navier–Stokes equations can be made dimensionless, and several possible choices exist. Here, we introduce next to  $\rho^*$  a reference length  $\ell^*$  a reference velocity  $U^*$  and a reference kinematic viscosity  $\nu^*$ . These base quantities together also define a reference time-scale  $\ell^*/U^*$ . If we now introduce

$$t = \frac{t^*}{(\ell^*/U^*)}; \quad x_i = \frac{x_i^*}{\ell^*}; \quad u_i = \frac{u_i^*}{U^*}; \quad p = \frac{p^*}{\rho^*(U^*)^2}, \quad (1.4)$$

then after some rewriting we may obtain the dimensionless incompressible fluid equations

$$\partial_j u_j = 0 \quad (1.5)$$

$$\partial_t u_i + \partial_j(u_i u_j) + \partial_i p - \frac{1}{\text{Re}} \partial_{jj} u_i = 0; \quad i = 1, 2, 3. \quad (1.6)$$

Here, we introduced the shorthand notations  $\partial/\partial t^* \rightarrow \partial_t$  and  $\partial/\partial x_j^* \rightarrow \partial_j$ . As a result of the scaling of the variables, the Reynolds number  $\text{Re}$  has been introduced and is defined as  $\text{Re} = (U^* \ell^*)/\nu^* = (\rho^* U^* \ell^*)/\mu^*$ .

We observe two different contributions to the time-derivative of the velocity fields in (1.6), called ‘fluxes’. The nonlinear term  $\partial_j(u_i u_j)$  and the gradient of pressure  $\partial_i p$  are known as convective fluxes, while the linear term  $\partial_{ji} u_i / \text{Re}$  is the viscous flux. The Reynolds number is the only dimensionless group that arises in the description of incompressible flow of Newtonian fluids. The Reynolds number is a measure of the ratio between the ‘destabilizing’ contributions arising from the convective terms compared to the ‘stabilizing’ effects due to the viscous terms [125]. Correspondingly, it comes as no surprise that turbulent flow may arise for sufficiently large  $\text{Re}$ , while strongly viscous ‘Stokes’ or ‘creeping’ flow corresponds to the limit of vanishing  $\text{Re}$ . We will discuss this at greater length momentarily.

### Conservation principle

The Navier–Stokes equations express a physical conservation principle which may be recognized from the fact that these equations can be written in divergence form. We introduce a shorthand notation for (1.6) as

$$\partial_t u_i = \partial_j f_{ji}, \quad (1.7)$$

with

$$f_{ji} = -\left( u_j u_i + p \delta_{ji} - \frac{1}{\text{Re}} \partial_j u_i \right), \quad (1.8)$$

in which  $\delta_{ji}$  denotes Kronecker’s delta, i. e.,  $\delta_{ji} = 1$  if  $j = i$  and  $\delta_{ji} = 0$  otherwise. If we integrate (1.7) over an arbitrarily fixed volume of fluid  $V$ , we find

$$\frac{d}{dt} \int_V u_i dV = \int_V \partial_t u_i dV = \int_V \partial_j f_{ji} dV = \int_{\partial V} f_{ji} n_j dS, \quad (1.9)$$

where  $\partial V$  denotes the boundary of  $V$  and  $\mathbf{n} = [n_1, n_2, n_3]$  is the outward unit normal on  $\partial V$ . Use was made of the divergence theorem of Gauss in the last step in (1.9). Equation (1.9) shows that the volume integral of  $u_i$  over  $V$  can only change in time due to fluxes across the boundary of  $V$ . This conservation property provides a basis for numerous spatial discretization methods, such as finite volume and finite element methods. Expression (1.9) provides an example of a so-called ‘weak’ formulation of the governing equations. The weak formulation expresses the fact that the equations of motion are only required to be satisfied in an integral sense. This relaxes some of the smoothness conditions that solutions to the differential form of the Navier–Stokes equations (1.6) have to satisfy. We will return to this in later chapters, e. g., Chapter 3 and Chapter 5.

### Kelvin theorem

Another important analytical property is the Kelvin theorem associated with the Navier–Stokes equations. This involves a line-integral with reference to evolving fluid loops. In fact, one has

$$\frac{d}{dt} \oint_{\Gamma(\mathbf{u})} u_i dx_i = \frac{1}{\text{Re}} \oint_{\Gamma(\mathbf{u})} \partial_{jj} u_i dx_i \quad (1.10)$$

for a closed fluid loop  $\Gamma(\mathbf{u})$  that moves with the Eulerian velocity  $\mathbf{u}(\mathbf{x}, t)$ . At the limit in which  $\text{Re} \rightarrow \infty$ , the integral of the velocity over  $\Gamma(\mathbf{u})$  is a constant of the motion. This is a basic property of solutions to the so-called Euler equations that emerge as the inviscid limit of the viscous Navier–Stokes formulation. The Kelvin theorem can be used to formulate regularized flow descriptions which share this conservation property with the Navier–Stokes system. It can serve as a basis for large-eddy modeling [51] to which we will return in Chapter 6.

### Transformation properties

The Navier–Stokes equations possess a number of transformation invariances and symmetries that play an important role in the flow dynamics [54, 199]. As an example, these invariances can be used to guide subgrid modeling that is consistent with generic properties of the basic flow equations [158]. In general, one considers transformations  $(\mathbf{x}, t) \rightarrow (\mathbf{X}, t)$  for which the Navier–Stokes equations are invariant. The most basic transformation with this property is the scaling that implies  $\mathbf{X} = a\mathbf{x}$  for a constant  $a$ . Consequently,  $\mathbf{U} = \dot{\mathbf{X}} = a\mathbf{u}$ , and one may readily verify the invariance of the equations under this transformation. Likewise, one may verify the invariance of the equations upon translation, i. e.,  $\mathbf{X} = \mathbf{x} - \mathbf{a}$  for a fixed shift of the origin  $\mathbf{a}$ . The equations also possess rotational symmetry. This may be expressed by the relationship  $X_i = A_{ij}x_j$ , where  $A$  is a fixed unitary matrix ( $\det(A) = 1$ ). The velocity transforms in the same way  $U_i = A_{ij}u_j$ , and the equations remain invariant under rotations. Finally, we mention the Galilean invariance of the Navier–Stokes equations defined through transformations of the type

$$\mathbf{X} = \mathbf{x} + \mathbf{V}t - \mathbf{a} \quad (1.11)$$

in which  $\mathbf{V}$  is a constant velocity difference between the two coordinate systems and  $\mathbf{a}$  is an initial shift of the origin. These four examples are only the better known transformation properties of the Navier–Stokes equations; further details and extensive studies of their consequences may be found in the literature (e. g., [83]). The relevance of such transformation and symmetry properties for large-eddy modeling lies in the consequences for proposed turbulence models in case one requires that the modeled equations also possess as many as possible of these properties.

### Burgers equation

Since the full system of Navier–Stokes equations can, in general, not be solved analytically, a mathematically much simpler model system is desired with which important basic properties of the governing equations can be effectively illustrated. Although properties of any simplified model system will deviate in some respects from the full system of equations, certain Navier–Stokes phenomena can still be understood and illustrated qualitatively at the level of the model system. For the Navier–Stokes equations, the viscous Burgers equation is a popular model system. In one spatial dimension, the Burgers equation reads

$$\partial_t u + \partial_x \left( \frac{1}{2} u^2 \right) - \frac{1}{\text{Re}} \partial_{xx} u = f, \quad (1.12)$$

in which  $f$  denotes a forcing term. The unforced equation can formally be solved analytically by suitably transforming the solution  $u$ . The Burgers equation displays a characteristic quadratic nonlinearity and a linear viscous contribution, which also arises in the full Navier–Stokes system, while the pressure gradient term is absent. This model system has been extensively studied. In particular, with a suitable forcing term  $f$ , (numerical) solutions can be obtained that share quite a number of properties with fully turbulent solutions governed by the complete system of Navier–Stokes equations. The study of these solutions and their relation with real turbulence is suggestively called ‘Burgulence’ in the literature [53].

### Compressible fluids

So far, we have considered incompressible fluids such as water. We next turn to compressible fluids that correspond to most common gases and mixtures such as air. In this case the fluid density is a function of location and time:  $\rho(\mathbf{x}, t)$ . In addition, an equation of state is required that relates pressure to density and temperature. Commonly, the ideal gas law is adopted for this relationship. Hence, for compressible flow, not only the gradient of the pressure is relevant, as in the incompressible case, but also the actual value of  $p$  is important. This extension also implies that, next to a reference density  $\rho^*$ , reference length  $\ell^*$ , reference velocity  $U^*$  and reference viscosity  $\mu^*$ , the introduction of a reference temperature  $T^*$  is required to render the governing equations in dimensionless form [222]. The dimensionless compressible flow equations can be expressed as

$$\partial_t \rho + \partial_j (\rho u_j) = 0 \quad (1.13)$$

$$\partial_t (\rho u_i) + \partial_j (\rho u_i u_j) + \partial_i p - \partial_j \sigma_{ij} = 0; \quad i = 1, 2, 3 \quad (1.14)$$

$$\partial_t e + \partial_j ((e + p) u_j) - \partial_j (\sigma_{ij} u_i) + \partial_j q_j = 0. \quad (1.15)$$

Here,  $e$  is the total energy density given by

$$e = \mathcal{E}(\rho, \mathbf{u}, p) = \frac{p}{\gamma - 1} + \frac{1}{2}\rho u_i u_i, \quad (1.16)$$

which introduces the function  $\mathcal{E}$  as a useful shorthand notation for later convenience when filtering these equations (see also [228]). In the definition of the energy density, we introduced  $\gamma = C_p/C_V$  as the ratio of the specific heats at constant pressure  $C_p$  and constant volume  $C_V$ , respectively. For air  $\gamma \approx 7/5$ .

In order to complete the compressible formulation, additional constitutive relationships need to be introduced. The viscous stress tensor  $\boldsymbol{\sigma}$ , for Newtonian fluids, is based on the temperature  $T$  and velocity vector  $\mathbf{u}$

$$\sigma_{ij} = \mathcal{F}_{ij}(\mathbf{u}, T) = \frac{\mu(T)}{\text{Re}} S_{ij}(\mathbf{u}); \quad i, j = 1, 2, 3, \quad (1.17)$$

where

$$S_{ij}(\mathbf{u}) = \partial_j u_i + \partial_i u_j - \lambda \delta_{ij} \partial_k u_k; \quad i, j = 1, 2, 3 \quad (1.18)$$

is the rate of strain tensor, and the shorthand notation using  $\mathcal{F}_{ij}$  will become clear when filtering the equations. In most applications it is common to set the parameter  $\lambda = 2/3$ , in which case  $S_{ij}$  is a traceless tensor.

The dimensionless viscosity  $\mu(T)$  that appears in (1.17) can be modeled in various ways. For flows that are nearly incompressible, one may adopt  $\mu = 1$ , while in more general cases it is a function of temperature  $T$ . A simple model that is frequently considered uses  $\mu(T) = T$ , whereas the dynamic viscosity for air is in good approximation parameterized by Sutherland's law

$$\mu(T) = T^{\frac{3}{2}} \frac{1 + C}{T + C}, \quad (1.19)$$

where the constant  $C$  is related to the reference temperature  $T^*$  that was used to render the compressible flow equations dimensionless. Commonly, this constant is set  $C = 110.4 (K)/T^*$ , where  $T^*$  is measured in Kelvin ( $K$ ). For common atmospheric conditions,  $T^* \approx 273 (K)$  and  $C \approx 0.4$ .

To complete the compressible formulation, the heat flux vector  $\mathbf{q}$  is given by

$$q_j = \mathcal{Q}_j(T) = -\frac{\mu(T)}{(\gamma - 1) \text{Re Pr } M^2} \partial_j T; \quad j = 1, 2, 3, \quad (1.20)$$

expressing  $q_j$  through the function  $\mathcal{Q}_j$  in terms of the temperature  $T$ . Here, we introduced the Prandtl number  $\text{Pr}$ . For air the Prandtl number is on the order of one, but a value of  $\text{Pr} \approx 0.72$  is commonly adopted. Moreover, we introduced the reference Mach number as  $M = U^*/c^*$ , where  $c^* = \sqrt{\gamma R^* T^*}$  is the reference value for the speed of sound in which  $R^*$  is the ideal gas constant. Finally, the temperature is related to the density and the pressure by the ideal gas law

$$T = \mathcal{T}(\rho, p) = \gamma M^2 \frac{p}{\rho}. \quad (1.21)$$

The Mach number is a measure for compressibility effects in a flow. As the Mach number approaches zero, the dynamics of the compressible flow equations approach the incompressible limit, whereas supersonic flows correspond to  $M > 1$ , and additional features such as shock-waves may arise.

### Hyperbolic conservation laws

The Navier–Stokes equations (1.13)–(1.15) are so called hyperbolic conservation laws. As in the incompressible counterpart (1.5)–(1.6), these equations contain viscous and convective contributions. The viscous terms are those that contain the stress tensor  $\sigma_{ij}$  or the heat-flux vector  $q_j$ . These are related to dissipative effects that represent the tendency to reduce rapid, strongly localized fluctuations. These terms involve second-order spatial derivatives. The remaining contributions that contain first-order spatial derivatives are the convective terms that constitute the strong nonlinear effects that are responsible for the complex evolution of turbulent flow. If we introduce the state-vector  $\mathbf{W} = [\rho, \rho u_i, e]$ , then the compressible Navier–Stokes equations can be written in a compact form as

$$\partial_t \mathbf{W} + \nabla \cdot \mathbf{f}_c - \nabla \cdot \mathbf{f}_v = 0, \quad (1.22)$$

where  $\mathbf{f}_c$  and  $\mathbf{f}_v$  contain the convective and the viscous flux-vector contributions respectively. These flux-vectors can be inferred from (1.13)–(1.15). The reason for identifying these two types of terms is not only related to the physical significance of these terms, but also to the fact that both impose specific and separate numerical requirements as will be clarified later.

The compressible flow equations play an important role as versatile points of departure in a number of application areas. At sufficiently low Mach numbers, their dynamics is in a number of aspects virtually identical to incompressible flows, while with increasing Mach number additional effects come into play, e. g., shock-waves that may arise as the flow becomes supersonic. These facts make this system of equations an appealing general model system for exposing various developments in direct and large-eddy simulation. For this reason, a number of descriptions and illustrations in this book will be based on the compressible formulation, although it is understood that those findings apply equally well to the incompressible case. The converse also applies, and we will move freely between either of these basic formulations in the remainder of this book and select the formulation that is most economical to illustrate a specific point.

To complete this section we sketch some examples in which the basic Navier–Stokes formulation is extended to describe further complicating effects that may be of relevance in specific applications. Usually, these extensions require the introduction

of additional terms in the equations or even additional equations that are dynamically coupled to the basic flow equations.

### Gravity-driven flow

The first class of extensions involves additional terms on the right-hand side of equation (1.22). These additional terms can be source terms, e. g., in case external body forces play a role. For example, buoyancy effects and gravity-driven currents can be represented through the introduction of such a source term in the momentum and energy equations. If  $g^*$  denotes the gravitational constant, then the equations can be written as

$$\partial_t \rho + \partial_j(\rho u_j) = 0 \quad (1.23)$$

$$\partial_t(\rho u_i) + \partial_j(\rho u_i u_j) + \partial_i p - \partial_j \sigma_{ij} = \frac{\rho g_i}{Fr^2} \quad (1.24)$$

$$\partial_t e + \partial_j((e + p)u_j) - \partial_j(\sigma_{ij}u_i) + \partial_j q_j = \frac{\rho g_j u_j}{Fr^2}, \quad (1.25)$$

where the gravitational acceleration  $\mathbf{g}^* = g^* [g_1, g_2, g_3]$ . As a result of introducing a new physical element in the formulation, a corresponding dimensionless group arises in the equations. In gravity-driven flows, this is the so-called Froude number given by  $Fr = U^* / \sqrt{g^* \ell^*}$ . Likewise, if electromagnetic interactions play a role in the evolution of a flow, additional source terms can be introduced to describe these effects. Such extensions of the equations with ‘source’ terms imply that the conservation property is no longer maintained. Another important extension of the basic equations arises by considering ‘external’ motions of the frame of reference. As an example, one may think of solid-body rotations that play an important role in various geophysical problems, e. g., in ocean-circulation modeling. If we consider rotation about a rotation-vector  $\boldsymbol{\omega}^*$ , then the Navier–Stokes equations require the introduction of an additional term  $2\mathbf{u}^* \times \boldsymbol{\omega}^*$ . The corresponding dimensionless group, in this case, is the so-called Rossby number that involves  $\omega^* = |\boldsymbol{\omega}^*|$  next to the reference quantities previously introduced.

### Active and passive scalars

The second class of extensions can be characterized as extensions that require the additional introduction of equations or systems of equation that are in some way dynamically coupled to the basic Navier–Stokes equations. One may think of applications in the field of combustion that imply the introduction of source terms in the Navier–Stokes equations, alongside additional equations that describe the particular combustion model and involve reaction product terms that incorporate the reaction rate and the enthalpy of formation of reaction products, among others [162]. Moreover, non-Newtonian flow behavior and dispersion phenomena may require such modeling. As

an example, we consider ‘passive’ and ‘active’ scalars. In the case of passive scalars, one commonly considers

$$\partial_t(\rho c) + \partial_j(u_j \rho c) - \frac{1}{Sc} \partial_{jj} c = 0, \quad (1.26)$$

where  $Sc$  denotes the so-called Schmidt number that characterizes molecular diffusive transport. The scalar field  $c$  is convected by the flow field  $u_j$ , and the finer features of  $c$  such as regions of large gradients are smoothed by the action of diffusion. Passive scalars can be used to quantify various aspects of turbulent mixing processes that may be relevant in process-engineering or relate to the spread of polluting agents. In Fig. 1.1 we depicted the evolution of the separating interface between the ‘upper’ and ‘lower’ parts of a shear layer as it transitions to turbulence [62]. The interface is defined as the isosurface  $c = 1/2$ . These scalar fields are also of more theoretical significance. Additional effects, such as the influence of local curvature on the evolution of the scalar, can be represented by introducing corresponding terms to (1.26).

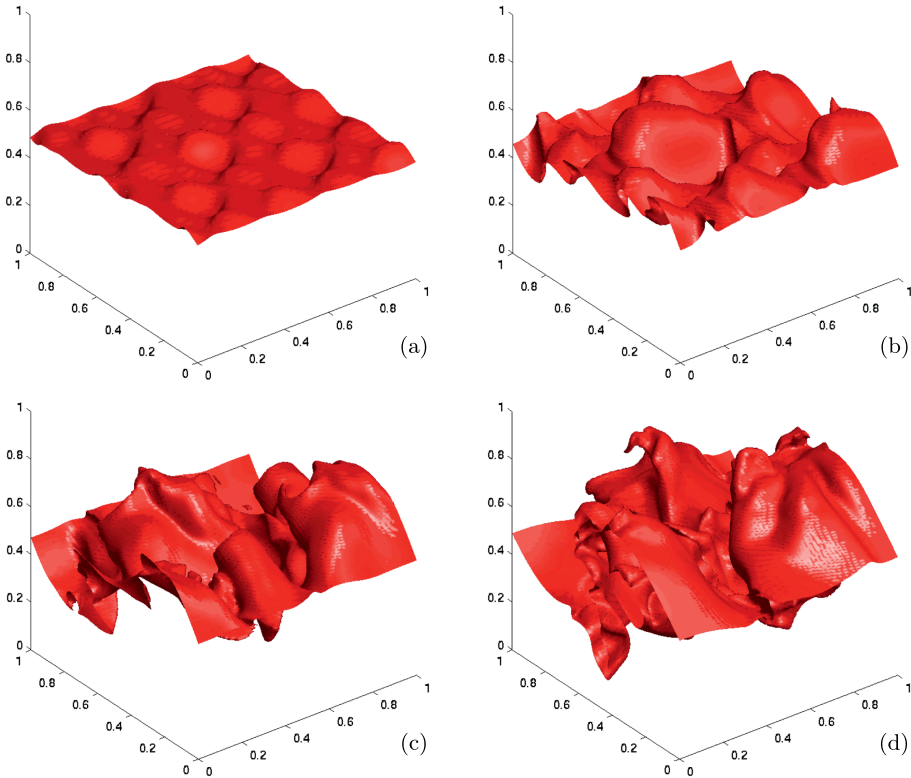


**Figure 1.1:** Evolution of separating interface between a passive ‘heavy’ fluid (top) and ‘lighter’ ambient fluid (bottom) at  $t = 10$  (a),  $t = 30$  (b),  $t = 60$  (c) and  $t = 100$  (d). The simulation was performed at a Schmidt number  $Sc = 10$ . From [62].

The coupling between the evolution of  $c$  and the flow field is only one-way, hence the term ‘passive’ scalar. Various flow problems, such as those associated with buoyancy effects, require additional coupling between the equation for the scalar and the Navier–Stokes equations giving rise to so-called two-way coupling models. This type of extensions involves the mutual interaction between, e. g., combustion, buoyancy or complex material properties and turbulence, and can give rise to strong turbulence modulation, which is an important field of applied and theoretical study. As an example, the effect of strong buoyancy is illustrated in Fig. 1.2, displaying the occurrence of interpenetrating ‘fingers’ of fluid. The influence of gravity on the evolving turbulent flow of an unstably stratified shear layer is quite striking in this case (compare with Fig. 1.1 which illustrates a passive scalar evolution).

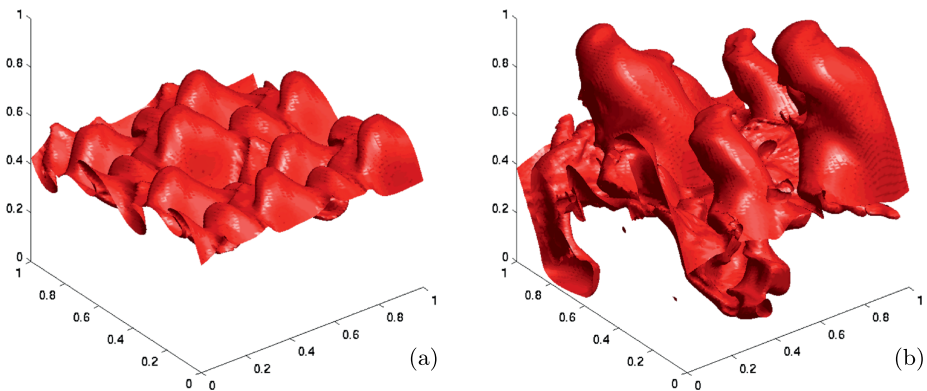


**Figure 1.2:** Snapshots of the separating interface between an active ‘heavy’ fluid (top) and ‘lighter’ ambient fluid (bottom) at  $t = 20$  (a) and  $t = 40$  (b) at  $Sc = 10$ . From [62].

### 1.3 Complexity reduction: options and limitations

In the previous section, the governing equations for fluid flow were introduced. Naively, one might think that, with the application of modern computers and proper numerical methods, turbulent flow problems would finally be resolved. Instead, one faces a well-known but still surprising deadlock. On the one hand, the basic physical principles and numerical formulations are available, but on the other hand, existing tools for analysis are not sufficiently powerful, and the required computational effort is typically so unrealistically high that it renders the necessary simulation studies unfeasible. Regarding the latter issue of computational effort, one could, instead, concentrate on simulation strategies in which the dynamic complexity of the flow is reduced. Conceivably, this could lead to formulations that would, at least, be feasible within the limits of present-day computers. Whether such a reduced description still satisfies the quality criteria posed by the application context is a matter that requires careful, problem-specific assessment.

In this section, we will therefore first sketch the backgrounds of some of the very high complexity solutions of turbulent flows. Then, we introduce and illustrate low-pass filters. While low-pass filtering is undoubtedly very effective in reducing the complexity of a signal and hence the cost associated with its accurate numerical representation, this filtering also leads to a potentially significant reduction in information content. Correspondingly, predictions based on filtered solutions will be less accurate and less complete. Whether this loss of accuracy is acceptable or not in a given application area needs to be considered with great care. After all, the goal is to obtain a proper balance between complexity reduction and retention of an adequate amount of flow detail for quantitative predictions. We will consider this central problem area in some detail in this section as well.

### Burgers flow complexity

The high complexity of turbulent flow solutions arises from the action of the nonlinear convective fluxes. This can be illustrated quite easily by turning to the unforced viscous Burgers equation (1.12). If we consider an initial state of the form  $u = \sin(kx)$ , with wave-number  $k$ , then we find from insertion into (1.12) a total flux which is given explicitly by

$$\partial_t u|_{t=0} = -\frac{k}{2} \sin(2kx) - \frac{k^2}{\text{Re}} \sin(kx). \quad (1.27)$$

We notice that there are two essentially different contributions to the flux. First, we see a contribution with wave number  $2k$  arising from the nonlinear convective flux. This will induce a component in the solution with wave number  $2k$  as well as the solution evolves. Second, the viscous flux gives a contribution with a wave number equal to that of the initial state. This contribution implies that the amplitude of the initial  $\sin(kx)$  will be reduced as the solution develops, but it will not alter its spectral content.

As time progresses, further wave numbers will emerge in the solution due to the continuing (self-)interactions between solution components of different wave numbers. If we consider any two Fourier modes from a Fourier series of the solution, e. g., modes  $\sim \exp(ik_1x)$  and  $\sim \exp(ik_2x)$  with wave-numbers  $k_1$  and  $k_2$ , then a convective flux with wave-number  $k_1 + k_2$  will emerge owing to the quadratic nature of the convective nonlinearity. This flux component will obviously contribute to the  $k_1 + k_2$  component in the evolving solution that gradually will become more complex, i. e., with more Fourier modes contributing significantly to the solution.

In Fig. 1.3 the evolution of the initial state  $u(x, 0) = \sin(2\pi x)$  is shown, subject to periodic boundary conditions. Clearly, as time progresses, the solution develops a sharp gradient, which corresponds to high values of the wave number, next to smooth parts in which the solution varies approximately linearly. The latter regions are associated with small values of the wave number. Thus, from an initial state with only

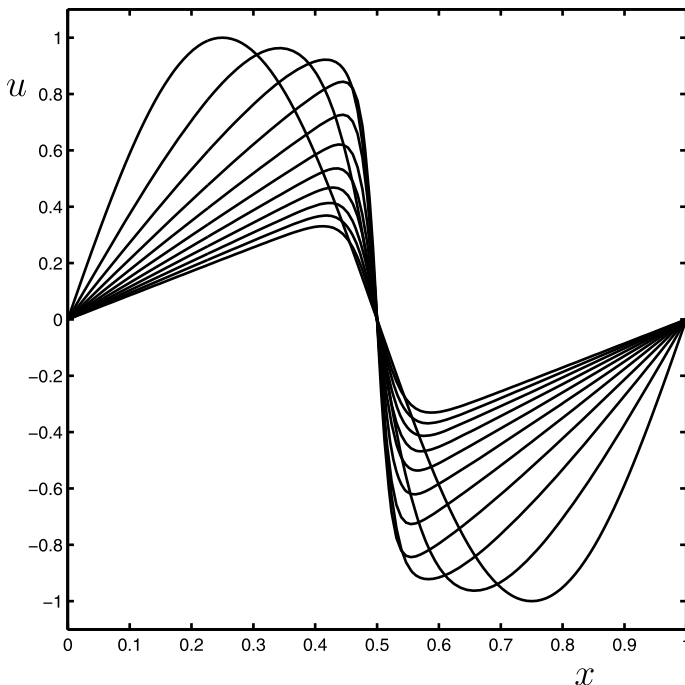


**Figure 1.3:** Evolution of the solution to the viscous Burgers equation at  $Re = 100$ . Shown are the initial condition  $u(x, 0) = \sin(2\pi x)$  (dashed), the intermediate solutions at  $t = 0.1, 0.2, 0.3, \dots$  (solid) and the solution at  $t = 1$  (dash-dotted).

one wave number, the evolving Burgers solution is characterized by a number of wave numbers that differ considerably in size. The ratio between the largest and the smallest relevant wave numbers is governed by the Reynolds number: As  $Re$  increases, so does this ratio, implying that smaller and smaller length scales become dynamically important with increasing  $Re$ . In the Burgers example, this leads to a sharper gradient in the middle of the domain as  $Re$  increases.

The ratio of the magnitude of the two fluxes in (1.12) depends on  $k$  and  $Re$ . We can identify two regimes in this explicit example. If  $k \ll Re/2$ , then the viscous flux is much smaller than the convective flux; clearly, structures with ‘large’ length scales (i. e., small  $k$ ) behave nearly inviscidly. On the other hand, if  $k \gg Re/2$ , then the  $k^2$ -dependence of the amplitude of the viscous flux will render this flux much larger than the convective flux. So, even if  $Re \gg 1$ , an almost purely dissipative dynamical behavior results for structures that are sufficiently localized in space.

### Three-dimensional flow complexity: energy-cascade

The Burgers example concisely illustrates the essential differences between convective and viscous fluxes. Quantitatively, however, the impression obtained from this

one-dimensional example is not accurate. Realistic three-dimensional turbulent flow fields possess a much more intricate structure in which simultaneously many more modes contribute significantly to the solution. The complexity of such turbulent solutions, however, still follows from the same basic action and interplay of convective and viscous fluxes as observed in the Burgers equation.

A realistic turbulent flow field contains (vortical) structures with many different length-scales, including a very wide spectrum of small-scale components [125, 171]. The length-scales of these components are much smaller than the length-scales that define the flow geometry, i. e., length-scales characteristic of the corresponding mean flow. Among these different structures, which we will loosely refer to as ‘eddies’, we can identify a hierarchy in the mean dynamical interactions. In particular, interactions among eddies with a comparably large length-scale (small  $k$ ) are approximately inviscid in nature and can give rise to eddies with smaller length-scales (higher  $k$ ). For example, one may think of events in which a comparably large structure disintegrates into a number of spatially more localized structures. This process of approximately inviscid interactions among eddies creates a whole variety of short and longer living dynamic structures of various length-scales up to structures that are spatially so localized that their motions are dominated by linear viscous actions.

The characteristic convective–viscous interactions give rise to a basic flow scenario that is known as the ‘energy-cascade’. In this scenario kinetic energy is transferred, on average, from the large to the smaller scales [112, 123]. This is referred to as ‘forward’ scatter. The reverse process can also arise: Within an evolving flow, locally situations may arise in which eddies with small length-scales can merge into eddies with a larger characteristic size. In this way, energy can also be transferred to larger-scale features that are known as ‘backscatter’ events. In actual turbulent flows, these backscatter events almost outweigh the ‘forward’ scatter events. However, the final statistical mean direction of energy flow is from the larger to the smaller scales [25, 53, 112].

In a turbulent flow, the energy-cascade is kept alive through external conditions, e. g., related to inflow perturbations or continuous agitation. The length-scales by which these external conditions provide forcing to the flow are assumed to be quite large and correspond to structures with approximately inviscid dynamics. As a result of the (self-)interactions just described, a complex turbulent flow can emerge from this forcing, with smaller and smaller structures appearing up to a length-scale at which viscous dissipation becomes dominant. The length-scale of the flow-features that are significantly influenced by dissipation (the tail of the spectrum at high  $k$ ) depends on the Reynolds number. An increase in  $Re$  corresponds to a reduction of the smallest dynamically relevant scale as was also noticed previously in relation to the Burgers equation.

Using dimensional analysis, Kolmogorov [112] obtained predictions of the smallest dynamically relevant dissipative flow feature  $\ell_d$ . He showed that the dissipative length-scale  $\ell_d \sim Re^{-3/4}$  in three dimensions. In homogeneous turbulence, a so-called

inertial range of length-scales is known to develop in between the forcing length scales and  $\ell_d$ . In this range, the kinetic energy spectrum displays a behavior proportional to  $k^{-5/3}$ . Roughly speaking, the inertial range of scales provides a ‘conveyor belt’ for the energy that was supplied to the flow at the large scales and that is dissipated as heat at scales on the order of  $\ell_d$ . Since general turbulent flows typically share several main characteristics with homogeneous flows in various (localized) regions of their flow domain, the Kolmogorov prediction for the scaling of  $\ell_d$  provides a useful guideline for the dynamic range in more general flows as well. This is known as the isotropy hypothesis.

### Degrees of freedom

In order to accurately capture all relevant features of a turbulent flow, it is clear that a representation is required that is capable of capturing the huge amount of information that is contained in the physical details of the flow. In a numerical treatment, the solution is ‘discretized’ which implies, among other things, that the continuous solution is approximated by a finite set of values corresponding as closely as possible to the values of the solution on a grid of discrete positions in physical space. This approach is followed, e. g., in finite difference methods [128]. Alternative representations exist in which one attempts to approximate the solution by expanding it with respect to an appropriate set of basis functions, e. g., in spectral [24] or finite element methods. Hence, in these approaches, one also approximates the continuous solution in terms of a finite set of values, i. e., the expansion coefficients of the solution relative to the adopted basis.

The complexity of the turbulent flow that is approximated depends strongly on the flow conditions. To characterize the degrees of freedom and consequently, the required amount of discrete values that is needed for an accurate approximation we introduce an ‘integral’ length-scale  $\ell$ , which is characteristic of the mean flow or of the flow geometry, next to the ‘dissipation’ scale  $\ell_d$ . We assume that  $\ell \gg \ell_d$ . Using Kolmogorov’s prediction for  $\ell_d$ , one has  $\ell/\ell_d \sim \text{Re}^{3/4}$ . To capture all features of the flow with sufficient detail, we assume that the basic method requires  $n$  grid-points per  $\ell_d$ . The value of  $n$  obviously depends on the specific numerical method. There is a consensus that  $n$  should range from 3 to 5 for most common methods in order to provide at least some accuracy with which the smallest structures are captured (we will return to this in more detail in later chapters). In three spatial dimensions, this implies the total required resolution, i. e., the number of grid points,

$$N = \left( \frac{\ell}{(\ell_d/n)} \right)^3 \sim n^3 \text{Re}^{9/4}, \quad (1.28)$$

which displays an essential scaling on Re. Similar estimates can be made for the number of basis functions that are required in spectral or finite element methods.